Applied Surface Science 258 (2012) 6069–6074

Contents lists available at SciVerse ScienceDirect

Applied Surface Science

journal homepage: www.elsevier.com/locate/apsusc

Chemical bath deposition of SnO_2 and Cd_2SnO_4 thin films

Hani Khallaf[a], Chia-Ta Chen[b,c], Liann-Be Chang[b,c], Oleg Lupan[a,d], Aniruddha Dutta[a,e], Helge Heinrich[a,e], Firoze Haque[a], Enrique del Barco[a], Lee Chow[a,b,c,e,*]

[a] Department of Physics, University of Central Florida, Orlando, FL 32816, USA
[b] Graduate Institute of Electro-Optical Engineering, Chang Gung University, Kweishan, Taoyuan 333, Taiwan
[c] Green Technology Research Center, Chang Gung University, Kweishan, Taoyuan 333, Taiwan
[d] Department of Microelectronics and Semiconductor Devices, Technical University of Moldova, 168 Stefan cel Mare Boulevard, MD-2004 Chisinau, Republic of Moldova
[e] Advanced Materials Processing and Analysis Centre, Department of Mechanical, Materials, and Aerospace Engineering, University of Central Florida, Orlando, FL 32816, USA

ARTICLE INFO

Article history:
Received 15 December 2011
Accepted 1 March 2012
Available online 7 March 2012

Keywords:
SnO_2
Cd_2SnO_4
Transparent conducting oxides
Thin films
Chemical bath deposition

ABSTRACT

A new approach of chemical bath deposition (CBD) of SnO_2 thin films is reported. Films with a 0.2 μm thickness are obtained using the multi-dip deposition approach with a deposition time as little as 8–10 min for each dip. The possibility of fabricating a transparent conducting oxide layer of Cd_2SnO_4 thin films using CBD is investigated through successive layer deposition of CBD-SnO_2 and CBD-CdO films, followed by annealing at different temperatures. High quality films with transmittance exceeding 80% in the visible region are obtained. Annealed CBD-SnO_2 films are orthorhombic, highly stoichiometric, strongly adhesive, and transparent with an optical band gap of ~4.42 eV. Cd_2SnO_4 films with a band gap as high as 3.08 eV; a carrier density as high as 1.7×10^{20} cm^{-3}; and a resistivity as low as 1.01×10^{-2} Ω cm are achieved.

1. Introduction

Transparent conducting oxides (TCOs) such as indium tin oxide (ITO) play an important role in solar cells, light emitting diodes, as well as other optoelectronic devices. Seeking alternatives to ITO has been the focus of attention for a long time due to the rising costs of indium. As a result, other TCO layers fabricated from ZnO, CdO, Cd_2SnO_4, and Zn_2SnO_4 are heavily investigated [1,2]. Although several techniques are currently in use to grow such layers, chemical bath deposition (CBD) presents a simple, low temperature, and inexpensive large-area deposition alternative. For over forty years, it has been widely used to grow wide-band gap group II–VI semiconducting thin films, such as CdS [3–9], CdO [10–14], and ZnO [15–20].

In a previous work [15], we have investigated CBD of ZnO using six different complexing agents, four of which proved to be successful in growing high quality ZnO undoped thin films with a band gap of 3.3 eV, a carrier density as high as 2.24×10^{19} cm^{-3}, and a resistivity as low as 6.48×10^{-1} Ω cm. More recently, we have succeeded to grow CBD-CdO thin films using three different complexing agents [14]. Annealed CdO undoped films with a band gap of 2.53 eV, a carrier density of ~1.89×10^{20} cm^{-3}, and a resistivity ~1.04×10^{-2} Ω cm were obtained.

SnO_2 thin films reported in the literature, however, have been obtained mainly by RF magnetron sputtering [21], metal organic chemical vapor deposition [22], vacuum evaporation [23], pulsed laser deposition [24], pulsed electron beam deposition [25], spray pyrolysis [26], sol–gel [27], chemical vapor deposition [28], and successive ionic layer adsorption and reaction [29]. However, very few attempts to grow SnO_2 thin films using CBD have been reported [30,31]. In both cases, the deposition time was of the order of several hours; 15–24 h in the work of Tsukuma et al. [30] and 5–12 h in the work of Supothina and De Guire [31]. Tsukuma et al. [30] reported a growth rate that ranged from 2 nm/h at 40 °C to 50 nm/h at 80 °C. Supothina and De Guire [31] reported growing SnO_2 films, 60–70 nm thick, after 12 h of deposition, with a growth rate of approximately 9 nm/h during the first 4 h. Clearly, the slow growth rate is a major limitation to using CBD as a viable technique to grow SnO_2 thin films.

In this work, we report a new approach of CBD-SnO_2 that enabled us to grow a 0.2 μm thick film using multi-dip deposition, with a deposition time as little as 8–10 min for each dip. We also investigate the possibility of fabricating a TCO layer of CBD-Cd_2SnO_4 thin film through growing CBD-CdO layer on top of the CBD-SnO_2 layer followed by heat treatments in air at different temperatures. Transmittance, reflectance measurements and band gap calculations are carried out for as-grown films as well as annealed films. Resistivity, carrier density, and Hall mobility of annealed

* Corresponding author at: Department of Physics, University of Central Florida, Orlando, FL 32816, USA.
E-mail address: Lee.Chow@ucf.edu (L. Chow).

0169-4332/$ – see front matter © 2012 Elsevier B.V. All rights reserved.
doi:10.1016/j.apsusc.2012.03.004

films are acquired at room temperatures using Hall effect measurements. Crystal structure as well as crystal quality of CBD-SnO_2 films are determined using X-ray diffraction (XRD), transmission electron microscopy (TEM), and Fourier transform infrared spectroscopy (FTIR). Film morphology, composition, and binding energy of CBD-SnO_2 are studied using atomic force microscopy (AFM) and scanning electron microscopy (SEM), Rutherford backscattering spectroscopy (RBS), and X-ray photoelectron spectroscopy (XPS), respectively.

2. Experimental details

SnO_2 films were prepared using aqueous solutions of tin chloride pentahydrate (0.028 M). Each bath contained 120 ml of de-ionized water (resistivity ~18.2 MΩ-cm) that was kept under stirring at 55 °C. Films were grown on 38 mm × 38 mm × 1 mm Schott Borofloat glass as well as quartz substrates. With the help of a Teflon holder, the glass substrate was kept vertically in the solution. The cleaning steps of the substrate are reported elsewhere [6]. To ensure deposition of high-quality and adhesive films, the substrate was removed from the solution whenever the solution becomes turbid and the homogeneous reaction starts to take place. The deposition time was about 8–10 min for each dip. In order to grow SnO_2 films with a ~0.2 μm thickness, the deposition process was repeated four consecutive times, with fresh solutions being used every time.

After annealing the SnO_2 film at 400 °C in air for 1 h, a 0.2 μm layer of CdO is grown on top of the SnO_2 layer using CBD. Both layers are then annealed at different temperatures in air. CdO thin films are grown using ammonia and ethanolamine as complexing agents, $CdSO_4$ as cadmium source $(NH_4)_2SO_4$ as a buffer, and H_2O_2 as an oxidation agent. Details of CBD of CdO thin films are reported elsewhere [14].

Specular transmittance measurements were carried out at room temperature in the wavelength range from 200 to 1200 nm, using a Cary 500 (Varian) double beam UV/vis spectrophotometer. Specular reflectance measurements were performed at an angle of incidence of 7° in the same wavelength range. The optical absorption coefficient α was calculated for each film using the equation [32]:

$$T = (1 - R)^2 \exp(-\alpha t) \quad (1)$$

where T is transmittance, R is reflectance, and t is film thickness.

The absorption coefficient α is related to the incident photon energy $h\nu$ as:

$$\alpha = \frac{K(h\nu - E_g)^{n/2}}{h\nu} \quad (2)$$

where K is a constant, E_g is the optical band gap, and n is equal to 1 for direct band gap material such as CdO. The band gap was determined for each film by plotting $(\alpha h\nu)^2$ versus $h\nu$ and then extrapolating the straight line portion to the energy axis. Resistivity, Hall mobility, and carrier density were evaluated by Hall effect measurements at room temperature in a Van der Pauw four-point probe configuration, using indium contacts, in an automated Hall effect system (Ecopia HMS-3000, Bridge Technology, Chandler Heights AZ, USA) with a 0.55 T magnetic induction. XRD was carried out using Rigaku D XRD unit (with 40 kV, 30 mA CuKα radiation, λ = 0.15406 nm). The sample was mounted at 2.5° and scanned from 20° to 80° in steps of 0.02° with a scan rate of 1.2° min^{-1}. TEM was performed using a Tecnai F30 STEM system operating at an acceleration voltage of 300 kV. Cross sections of CdO films were prepared with FEI 200 focused ion beam system. SEM micrographs were obtained using a JEOL 6400F SEM at an acceleration voltage of 10 kV. The FTIR micro-analysis was performed at room temperature using contact ATR optimized objective that covers a range of wavenumbers from 650 cm^{-1} to 4000 cm^{-1}. RBS measurements were acquired using a 2.25 MeV α-particles IONIX 1.7 MU Tandetron, with a surface barrier detector with energy resolution ≤15 keV (full width at half maximum – FWHM), positioned at a scattering angle of 165°. XPS was performed on a Physical Electronics PHI 5400 ESCA using unmonochromated Mg Kα radiation at 1253.6 eV. Each of the XPS spectra was acquired from 30 repeated sweeps. XPS Spectra were corrected from charging effects by referencing the adventitious C 1s peak to 284.6 eV. AFM images were acquired using Veeco Multimode SPM in tapping mode.

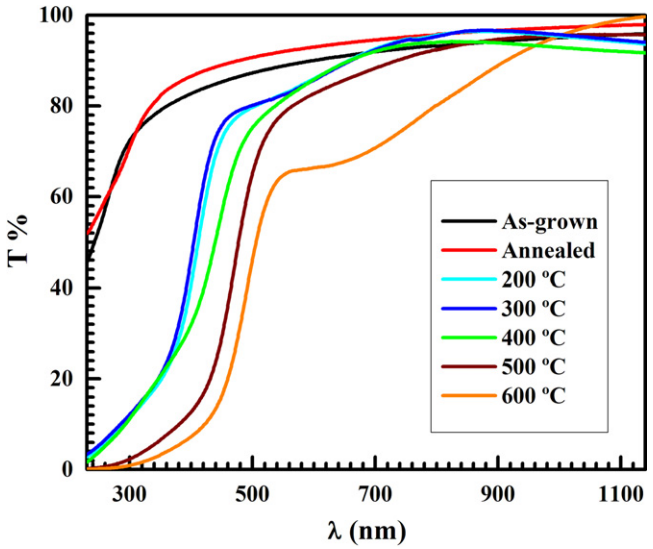

Fig. 1. Specular transmittance of as-grown and annealed SnO_2 films as well as Cd_2SnO_4 films annealed at 200–600 °C.

3. Results and discussion

It was observed that as-grown SnO_2 films are extremely adhesive, where highly concentrated sulfuric acid (98%) and nitric acid (96%) could not etch them. Therefore, in order to perform optical measurements, two substrates were tightly mounted together on the Teflon sample holder to ensure deposition on only one side of the substrate. Film thickness was determined using TEM, as will be shown later. Fig. 1 shows the optical transmittance of as-grown and annealed SnO_2 films as well as CdO + SnO_2 films annealed at 200, 300, 400, 500 and 600 °C. As shown, all films exhibit high transmittance that, in most cases, exceeds 80% in the visible region. A red shift in the optical absorption edge is observed due to formation of Cd_2SnO_4, which increases with increasing annealing temperature. The sharp absorption edge observed in Cd_2SnO_4 layers indicates that films still maintain high quality, even after annealing at temperatures as high as 600 °C. Films annealed at higher temperatures did not maintain the same quality and were discarded from any further characterizations. We have previously reported similar thermal-induced degradation of some CBD-ZnO and CBD-CdO films [14,15] that was attributed to stress in as-grown layers which caused films to lose their integrity after annealing, even at temperatures as low as 200–300 °C [15]. Since SnO_2 films initially annealed at 400 °C maintained their integrity as will be shown later in this work, it is likely that the CdO top-layer is responsible for this degradation. However, because CBD-SnO_2 films grown in this work were not separately subjected to heat treatments at temperatures higher than 400 °C, we cannot rule out the possibility of thermal-induced degradation of this layer at higher temperatures. Furthermore, growing CdO layer on top of SnO_2 using CBD typically exposes the SnO_2 film to a high pH environment due to

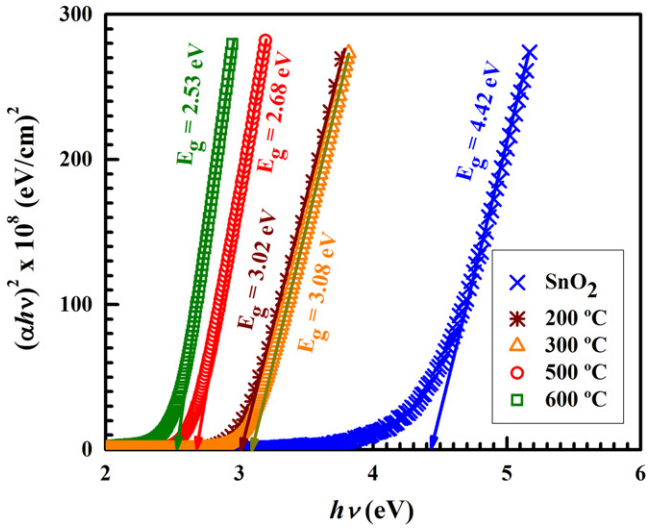

Fig. 2. Optical band gap calculations of SnO_2 films annealed at 400 °C as well as Cd_2SnO_4 films annealed at 200–600 °C.

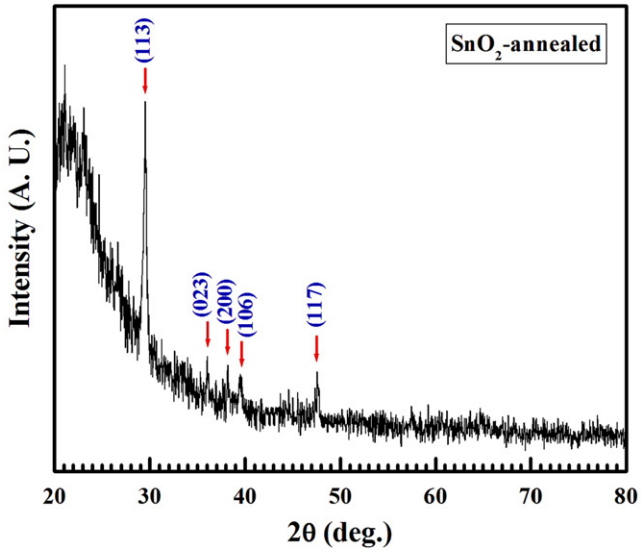

Fig. 3. XRD pattern of annealed SnO_2 film.

the high alkalinity of the solutions used, which may have a deep impact on the integrity of the SnO_2 bottom-layer. We have faced this challenge in a previous work when we tried to grow thick ZnO layers using the multi-dip deposition approach. We found out that any attempt to dip the original film in a fresh solution to grow another layer of ZnO resulted in immediate etching of the original layer followed by deposition of a non-uniform and porous new ZnO layer with inferior quality [15]. Although, such etching was not observed in this work, we cannot rule out the possibility of formation of cracks in the SnO_2 layer when dipped in the CdO-based solution. A future work will be dedicated to study this complex issue in detail.

Fig. 2 shows the optical band gap calculated for annealed SnO_2 films as well as Cd_2SnO_4 films annealed at different temperatures. The transmittance data shown in Fig. 1 and the corresponding reflectance data (not shown in this work) were used to calculate the absorption coefficient according to Eq. (1). As shown, band gap values of 4.42 eV, 3.02, 3.08, 2.68 eV, and 2.53 eV are observed for SnO_2 films annealed at 400 °C and Cd_2SnO_4 films annealed at 200, 300, 500, and 600 °C, respectively. The band gap calculated for films annealed at 400 °C is 2.83 eV. It is worth noting that the band gap we observed for CdO films annealed at 400 °C is 2.53 eV [14]. It should also be noted that, although the typical band gap of SnO_2 is around 3.75 eV [1], much higher values have been reported in the literature. Rakhshani et al. [33] reported a direct band gap of 4.11 eV, while Dawar and Joshi [34] reported band gap values in the range of 3.9–4.6 eV for SnO_2 thin films. On the other hand, Nozik [35], who was the first to prepare amorphous Cd_2SnO_4 films by RF sputtering, reported band gap values ranging from 2.06 eV to 2.85 eV for sputtered Cd_2SnO_4 films, depending on films conductivity. He also reported that the conductivity increase of Cd_2SnO_4 films is accompanied by a large shift of the fundamental optical absorption edge toward the UV. This was confirmed by the observations of Mamazza et al. [2], where a 15% rise in charge carrier density increased the optical band gap of Cd_2SnO_4 films from 2.97 eV to 3.18 eV. Coutts et al. [1] reported typical band gap values of Cd_2SnO_4 films of about 3.1 eV. As will be shown later, Hall measurements of annealed films, in accordance with the observations of Nozik [35] and Mamazza et al. [2], may give an explanation for the significant red-shift observed in Fig. 2 for Cd_2SnO_4 films annealed at temperatures higher than 400 °C. However, other factors such as SnO_2 film degradation and formation of secondary phases due to annealing cannot be ruled out.

The XRD pattern of annealed SnO_2 films is shown in Fig. 3. Annealed films are polycrystalline with a major (1 1 3) reflection and four weak reflections characteristic of the (0 2 3), (2 0 0), (1 0 6), and (1 1 7) planes of orthorhombic SnO_2 [36]. As grown SnO_2 films are found to be amorphous. In order to rule out the formation of secondary phases such as tin hydroxide during film deposition, FTIR measurements were carried out for both as-grown and annealed films. FTIR absorption measurements shown in Fig. 4 are identical for both films, where the broadband around 3300 cm^{-1} typically assigned to the O—H stretching mode of the hydroxyl group has not been detected. Such band was detected for both CBD-CdO and CBD-ZnO as-grown films [14,15]. Absorbance peaks observed between 650 cm^{-1} and 1500 cm^{-1} are due to Si—O and B—O stretching vibrations [37] originating from the "Borofloat" glass substrate. It is worth noting that the boron content in "Borofloat" glass is about 5.2%. XRD measurements of annealed Cd_2SnO_4 films revealed that all films are amorphous. According to Wu et al. [38], Cd_2SnO_4

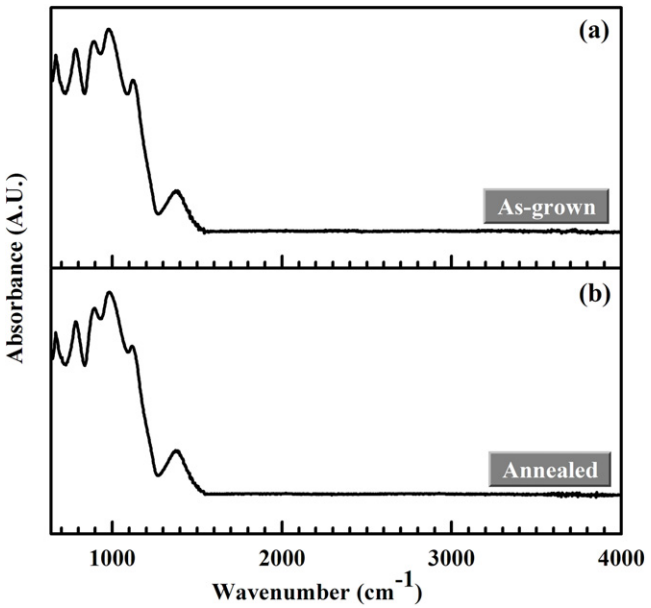

Fig. 4. FTIR absorbance spectrum of (a) as-grown SnO_2 film and (b) annealed SnO_2 film.

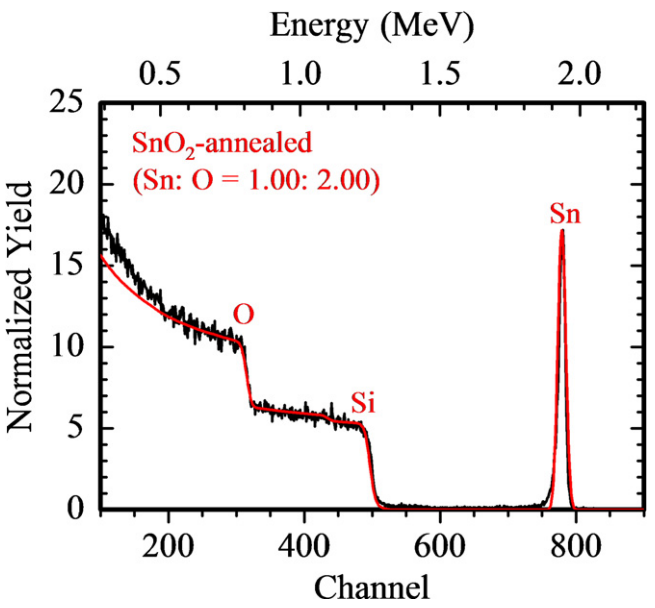

Fig. 5. RBS spectrum and RUMP simulation of annealed SnO_2 film.

films grown by RF magnetron sputtering start to crystallize at an annealing temperature of about 580 °C. Mamazza et al. [2], on the other hand, reported that Cd_2SnO_4 films deposited by RF magnetron co-sputtering from cadmium oxide and tin oxide targets in argon ambient begin to crystallize at an annealing temperature of about 525 °C. In this work, however, there was no indication of film crystallization, even after annealing at temperatures as high as 600 °C.

Fig. 5 shows the RBS spectra of annealed SnO_2 film. Simulation using Rutherford universal manipulation program (RUMP) [39] was implemented to obtain the best possible match to the raw RBS spectra. As shown, the film is highly stoichiometric with a Sn:O ratio of about (1.00:2.00). The XPS multiplex spectra of the Sn $3d_{5/2}$ and $3d_{3/2}$ peaks of annealed SnO_2 film is shown in Fig. 6(a). As shown, Sn $3d_{5/2}$ and $3d_{3/2}$ peaks of the annealed film are located at 486.4 eV and 494.8 eV which agrees well with the 8.41 eV spin-orbit energy splitting between Sn $3d_{5/2}$ and $3d_{3/2}$ states [40]. Also, the observed binding energy of 486.4 eV of Sn $3d_{5/2}$ lies within the accepted range of binding energy values for SnO_2 [40]. Fig. 6(b) shows the XPS multiplex spectra of the O 1s peak of annealed SnO_2 film. The O 1s peak of annealed film is located at 530.3 eV, which lies within the 527.7–530.6 eV range characteristic of O^{2-} oxides [40,41].

2-D and 3-D AFM images of as-grown as well as annealed SnO_2 film are shown in Figs. 7 and 8, respectively. Both films are continuous, uniform, and relatively smooth. The surface features of the films are comparable and the calculated surface roughness values are ~37.5 nm and 26.8 nm, for as-grown and annealed SnO_2 films respectively. Clearly, annealing reduced film roughness. Occasional crystallite overgrowth is observed on film surface, as revealed by SEM images (inset of Fig. 7b). This is attributed to colloidal particulates formed in solution and then adsorbed on the film. We have previously reported similar observations for CdS, CdO, and ZnO thin films grown by CBD [5,14,15].

HRTEM image of annealed SnO_2 film is shown in Fig. 9. As shown, the SnO_2 layer is about 0.20 μm thick. Film surface is smooth, in accordance with the AFM and SEM observations. Furthermore, SnO_2 layer is uniform with only small variations in film thickness being observed. The small area electron diffraction (SAED) pattern observed (insert of Fig. 9) confirms that SnO_2 film is polycrystalline with orthorhombic crystal lattice structure.

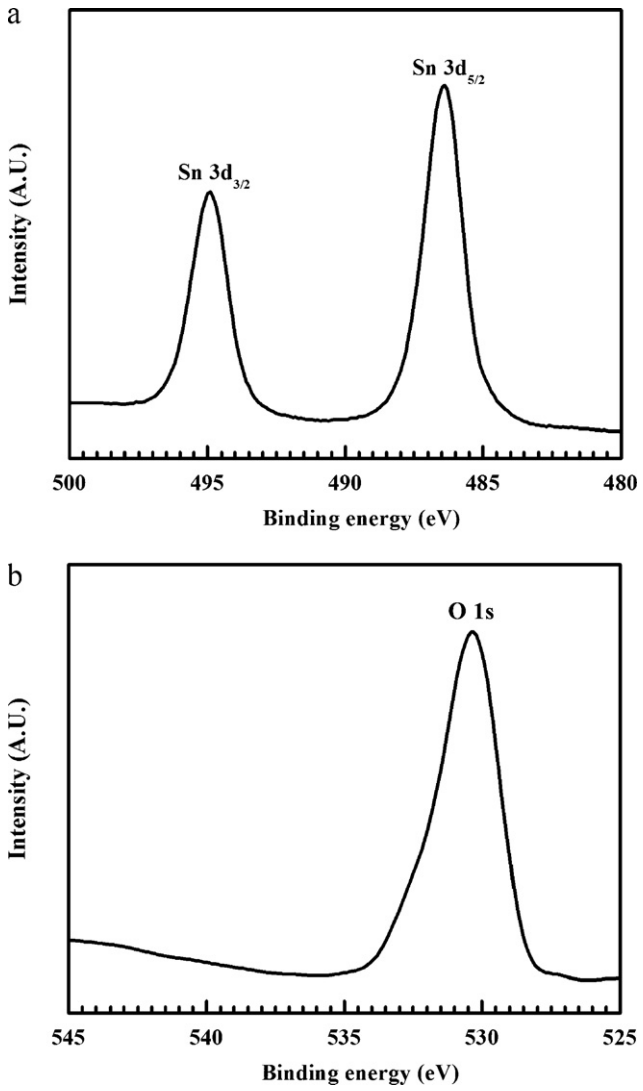

Fig. 6. XPS multiplex spectra of (a) Sn 3d and (b) O 1s of annealed SnO_2 film.

Table 1 shows a summary of Hall effect measurements and band gap calculations carried out at room temperature for SnO_2 film annealed at 400 °C, and Cd_2SnO_4 films annealed at 200–600 °C. The typical carrier density and resistivity values obtained for annealed SnO_2 films are of the order of 10^{12} cm^{-3} and 10^3 Ω cm, respectively. Comparing these values with their counterparts acquired for Cd_2SnO_4 films, it is clear that while the carrier density increased by 6–8 orders of magnitude, the resistivity of Cd_2SnO_4 films is only 4–5 orders of magnitude lower than that of SnO_2, depending on annealing temperatures. This has to do with the low mobility of amorphous Cd_2SnO_4 films compared to the much higher (2–3 orders of magnitude) mobility obtained for polycrystalline SnO_2 films. Hall mobilities as high as 65 ($cm^2\,V^{-1}\,s^{-1}$) were achieved by Wu et al. [38] for Cd_2SnO_4 films annealed in argon ambient. They have shown that electron mobility increases with increasing film crystallinity and concluded that annealing in a reducing atmosphere not only raises the free electron concentration but also increases electron mobility. They have reported film resistivity as low as 1.28×10^{-4} Ω cm. Nozik [35], on the other hand, reported that heat treatment in H_2 ambient at 280 °C for 10 min caused a significant reduction of film resistivity, where a sheet resistance as low as 2.3 Ω/sq was achieved. Mamazza et al. [2] reported 15% increases in carrier density for films subsequently annealed in H_2 after being annealed in He ambient. In this work, however, all samples were

Table 1
Hall effect measurements and optical band gap calculations carried out at room temperature for SnO_2 films annealed at 400 °C, and Cd_2SnO_4 films annealed at 200–600 °C.

Sample	Annealing temperature (°C)	E_g (eV)	Carrier density (cm^{-3})	Mobility ($cm^2\ V^{-1}\ s^{-1}$)	Resistivity (Ω cm)
SnO_2	400	4.42	5.15×10^{12}	1.61×10^{2}	7.53×10^{3}
Cd_2SnO_4	200	3.02	1.13×10^{20}	2.97×10^{0}	1.84×10^{-2}
Cd_2SnO_4	300	3.08	1.15×10^{20}	5.21×10^{0}	1.04×10^{-2}
Cd_2SnO_4	400	2.83	1.70×10^{20}	3.62×10^{0}	1.01×10^{-2}
Cd_2SnO_4	500	2.68	3.74×10^{19}	3.49×10^{-1}	4.78×10^{-1}
Cd_2SnO_4	600	2.53	2.86×10^{18}	1.17×10^{-1}	1.86×10^{1}

annealed in air. The highest carrier density and lowest resistivity achieved are $1.7 \times 10^{20}\ cm^{-3}$ and $1.01 \times 10^{-2}\ \Omega$ cm, respectively. Subsequent heat treatments in reducing atmospheres will be investigated in a future work.

Finally, comparing the band gap values with the corresponding carrier density of annealed films, it is obvious that the decrease in carrier density is responsible for the red shift observed in Fig. 1. As shown, films annealed at 200 and 300 °C which have very close carrier density values almost share the same absorption edge. Furthermore, at annealing temperatures higher than 400 °C, the band gap clearly decreases with decreasing carrier density. These observations agree well with the observations of Nozik [35] and Mamazza et al. [2]. However, such dependence on carrier density cannot explain the red shift observed for films annealed at 400 °C. In addition, it is noted that as the annealing temperature increases, the band gap values start to get closer to that of CBD-CdO films [14]. As a result, other factors such as SnO_2 film degradation and formation of secondary phases due to annealing cannot be ruled out.

Clearly, using a simple technique like CBD, we have succeeded to grow Cd_2SnO_4 layers with band gap values as high as 3.08 eV; a carrier density as high as $1.7 \times 10^{20}\ cm^{-3}$; and a resistivity as low as $1.01 \times 10^{-2}\ \Omega$ cm. Nevertheless, with the goal of reaching a resistivity of the order of $10^{-4}\ \Omega$ cm, more work toward optimizing both deposition and annealing of CBD-Cd_2SnO_4 thin films is required, in order to obtain a viable CBD-TCO layer. This work merely reports a preliminary step toward using CBD to fabricate a TCO layer of Cd_2SnO_4. Careful studies of post-heat treatments using different ambient such as He, Ar, and H_2; as well as thorough investigations of CBD-Cd_2SnO_4 film crystallinity, stoichiometry, and composition as a function of annealing temperature are still needed to achieve this goal.

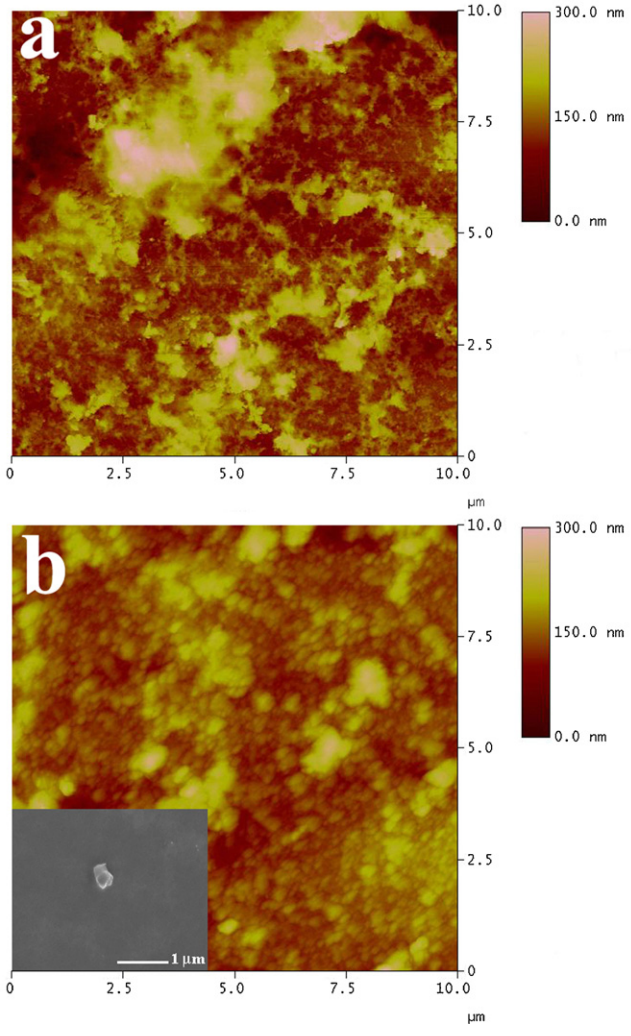

Fig. 7. 2D AFM images and SEM micrograph (inset) of (a) as-grown SnO_2 film and (b) annealed SnO_2 film.

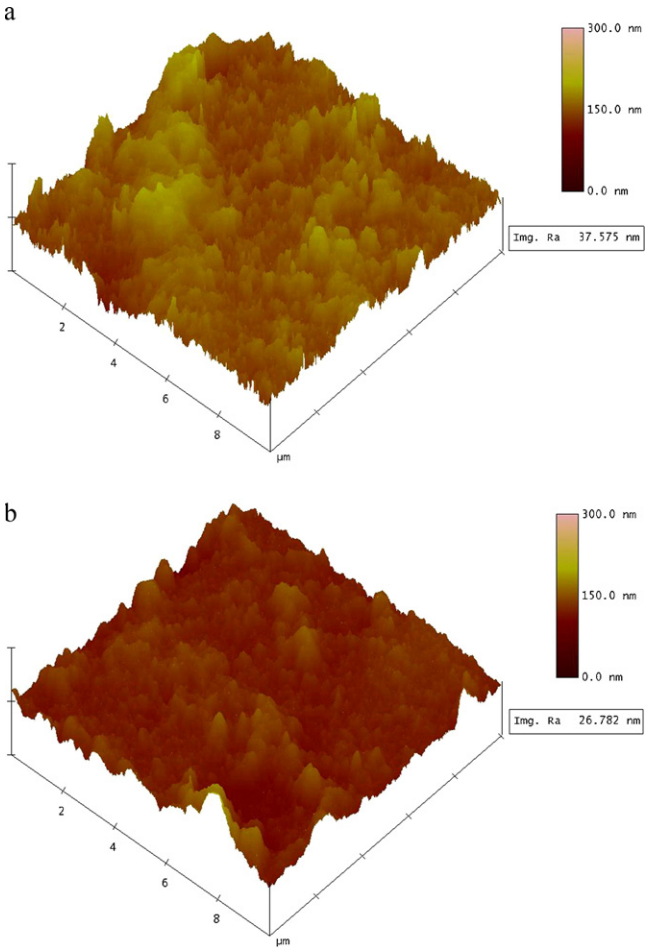

Fig. 8. 3D AFM images of (a) as-grown SnO_2 film and (b) annealed SnO_2 film.

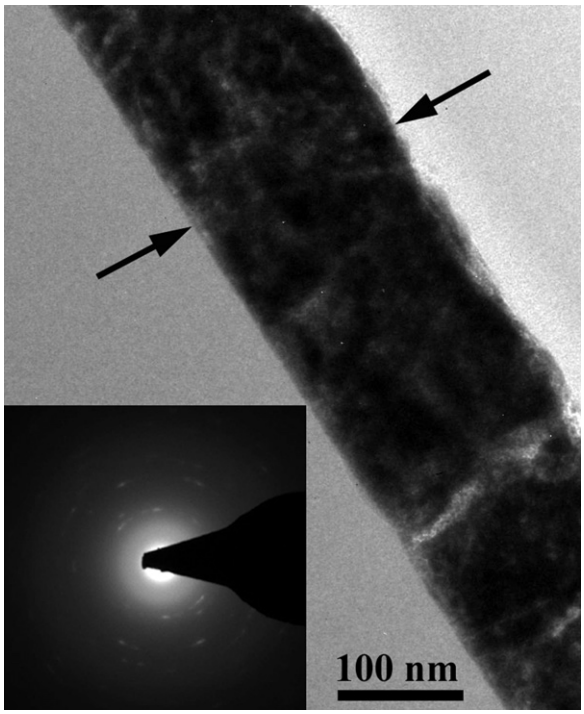

Fig. 9. HRTEM and TEM diffraction pattern (inset) of annealed SnO_2 film.

4. Conclusion

CBD of SnO_2 as well as Cd_2SnO_4 is investigated. A 0.2 μm thick CBD-SnO_2 films are grown using multi-dip deposition, with a deposition time as little as 8–10 min. Films are extremely adhesive and cannot be etched using concentrated sulfuric or nitric acid. Films are highly transparent with a band gap of ~4.42 eV and a transmittance exceeding 80% in the visible region of the spectrum. Annealed films are orthorhombic with a preferred orientation along the [1 1 3] direction. According to RBS data, annealed film is highly stoichiometric with a Sn:O ratio of ~1.00:2.00. AFM images show as-grown and annealed SnO_2 films to be continuous, uniform, and relatively smooth. An average roughness of ~37.5 and 26.8 nm is estimated for as-grown and annealed films, respectively. The electron diffraction pattern observed under TEM confirms that SnO_2 film is polycrystalline with orthorhombic crystal lattice structure.

Cd_2SnO_4 films with an optical band gap as high as 3.08 eV; a carrier density as high as 1.7×10^{20} cm^{-3}; and a resistivity as low as 1.01×10^{-2} Ω cm are obtained using CBD. Although promising, we believe that further work is needed to reach a resistivity of the order of 10^{-4} Ω cm, in order to fabricate a viable CBD-TCO layer. Careful studies of post-heat treatments as well as doping investigations [6,42,43] could lead to further improvement of the conductivity.

Acknowledgments

We are grateful to K. Scammon of the Advanced Materials Processing and Analysis Center (AMPAC), University of Central Florida, for his help with the XPS and RBS measurements. We are also grateful to Prof. Aravinda Kar and Mr. G. Lim of College of Optics and Photonics, University of Central Florida, for their help with the Hall measurements, and Prof. Alfons Schulte and his group, especially Mr. Sanghoon Park, of the Department of Physics, University of Central Florida, for their help with the FTIR measurements. This work was partially supported by USDA award # 58-3148-8-175, Apollo Technologies, Inc. and Florida High Tech. Corridor Council.

References

[1] T. Coutts, D. Young, X. Li, W. Mulligan, X. Wu, J. Vac. Sci. Technol. A 18 (2000) 2646.
[2] R. Mamazza, D. Morel, C. Ferekides, Thin Solid Films 484 (2005) 26.
[3] G. Kitaev, A. Uritskaya, S. Mokrushin, Russ. J. Phys. Chem. 39 (1965) 1101.
[4] I.O. Oladeji, L. Chow, J. Electrochem. Soc. 144 (1997) 2342.
[5] H. Khallaf, I. Oladeji, L. Chow, Thin Solid Films 516 (2008) 5967.
[6] H. Khallaf, G. Chai, O. Lupan, L. Chow, S. Park, A. Schulte, J. Phys. D: Appl. Phys. 41 (2008) 185304.
[7] I. Kaur, D. Pandya, K. Chopra, J. Electrochem. Soc. 127 (1980) 943.
[8] H. Khallaf, I. Oladeji, L. Chow, Thin Solid Films 516 (2008) 7306.
[9] J.M. Dona, J. Herrero, J. Electrochem. Soc. 144 (1997) 4081.
[10] M.Z. Najdoski, I.S. Grozdanov, B. Minceva-Sukarova, J. Mater. Chem. 6 (1996) 761.
[11] M. Ortega, G. Santana, A. Morales-Acevedo, Solid State Electron. 44 (2000) 1765.
[12] M. Ocampo, A.M. Fernandez, P.J. Sebastian, Semicond. Sci. Technol. 8 (1993) 750.
[13] L. de León-Gutiérrez, J. Cayente-Romero, J. Peza-Tapia, E. Barrera-Calva, J. Martínez-Flores, M. Ortega-López, Mater. Lett. 60 (2006) 3866.
[14] H. Khallaf, C.-T. Chen, L.-B. Chang, O. Lupan, A. Dutta, H. Heinrich, A. Shenouda, L. Chow, Appl. Surf. Sci. 257 (2011) 9237.
[15] H. Khallaf, G. Chai, O. Lupan, H. Heinrich, S. Park, A. Schulte, L. Chow, J. Phys. D: Appl. Phys. 42 (2009) 135304.
[16] P. O'Brien, T. Saeed, J. Knowles, J. Mater. Chem. 6 (1996) 1135.
[17] M. Ortega-López, A. Avila-García, M. Albor-Aguilera, V. Resendiz, Mater. Res. Bull. 38 (2003) 1241.
[18] A. Ennaoui, M. Weber, R. Scheer, H. Lewerenz, Solar Energy Mater. Solar Cells 54 (1998) 277.
[19] A. Drici, G. Djeteli, G. Tchangbedji, H. Derouiche, K. Jondo, K. Napo, J. Bernède, S. Ouro-Djobo, M. Gbagba, Phys. Status Solidi (a) 201 (2004) 1528.
[20] J.B. Chu, S.M. Huang, D.W. Zhang, Z.Q. Bian, X.D. Li, Z. Sun, X.J. Yin, Appl. Phys. A 95 (2009) 849.
[21] T. Minami, J. Vac. Sci. Technol. A 17 (1999) 1765.
[22] D. Liu, Q. Wang, H. Chang, H. Chen, J. Mater. Res. 10 (1995) 1516.
[23] C. Kaito, Y. Saito, J. Cryst. Growth 79 (1986) 403.
[24] F. Lamelas, S. Reid, Phys. Rev. B 60 (1999) 9347.
[25] R. Choudhary, S. Ogale, S. Shinde, V. Kulkarni, T. Venkatesan, K. Harshavardhan, M. Strikovski, B. Hannoyer, Appl. Phys. Lett. 84 (2004) 1483.
[26] R. Ayouchi, F. Martin, J. Barrado, M. Martos, J. Morales, L. Sánchez, J. Power Sources 87 (2000) 106.
[27] N. Baik, G. Sakai, N. Miura, N. Yamazoe, Sens. Actuators B 63 (2000) 74.
[28] R. Ghoshtagor, J. Electrochem. Soc. 125 (1978) 110.
[29] N. Deshpande, J. Vyas, R. Sharma, Thin Solid Films 516 (2008) 8587.
[30] K. Tsukuma, T. Akiyama, H. Imai, J. Non-Cryst. Solids 210 (1997) 48.
[31] S. Supothina, M. De Guire, Thin Solid Films 371 (2000) 1.
[32] J. Pankove, Optical Processes in Semiconductors, Dover Publications, New York, 1971.
[33] A. Rakhshani, Y. Makdisi, H. Ramazaniyan, J. Appl. Phys. 83 (1998) 1049.
[34] A. Dawar, J. Joshi, J. Mater. Sci. 19 (1984) 1.
[35] A.J. Nozik, Phys. Rev. B 6 (1972) 453.
[36] Joint Committee on Powder Diffraction Standards, Powder Diffraction File No. 078-1063.
[37] P. Pascuta, R. Lungu, I. Ardelean, J. Mater. Sci.: Mater. Electron. 21 (2010) 548.
[38] X. Wu, W. Mulligan, T. Coutts, Thin Solid Films 286 (1996) 274.
[39] L. Doolittle, Nucl. Instrum. Methods B 15 (1986) 227.
[40] J. Moulder, W. Stickle, P. Sobol, K. Bomben, in: J. Chastain (Ed.), Handbook of X-Ray Photoelectron Spectroscopy, Perkin-Elmer Corporation, Minnesota, 1992.
[41] J. Dupin, D. Gonbeau, P. Vinatier, A. Levasseur, Phys. Chem. Chem. Phys. 2 (2000) 1319.
[42] H. Khallaf, G. Chai, O. Lupan, L. Chow, S. Park, A. Schulte, Appl. Surf. Sci. 255 (2009) 4129.
[43] H. Khallaf, G. Chai, O. Lupan, L. Chow, H. Heinrich, S. Park, A. Schulte, Physica Status Solidi (a) 206 (2009) 256.